energies

MDPI

Article

Exploring the Environmental Benefits of an Open-Loop Circular Economy Strategy for Automotive Batteries in Industrial Applications

Luca Silvestri [1,*], Antonio Forcina [2], Cecilia Silvestri [3], Gabriella Arcese [1] and Domenico Falcone [4]

[1] Department of Engineering, University of Rome "Niccolò Cusano", Via Don Carlo Gnocchi, 3, 00166 Rome, Italy; gabriella.arcese@unicusano.it
[2] Department of Engineering, University of Naples "Parthenope", Isola C4, Centro Direzionale Napoli, 80133 Naples, Italy; antonio.forcina@uniparthenope.it
[3] Department of Economics, Engineering, Society and Business Organization, University of "Tuscia" of Viterbo, Via del Paradiso, 47, 01100 Viterbo, Italy; c.silvestri@unitus.it
[4] Department of Civil and Industrial Engineering, University of Cassino and Southern Lazio, 03043 Cassino, Italy; falcone@unicas.it
* Correspondence: luca.silvestri@unicusano.it

Abstract: Battery energy storage systems (BESSs) can overwhelm some of the environmental challenges of a low-carbon power sector through self-consumption with standalone photovoltaic (PV) systems. This solution can be adapted for different applications such as residential, commercial, and industrial uses. Furthermore, the option to employ second-life batteries derived from electric vehicles represents a promising opportunity for preserving the environment and improving the circular economy (CE) development. Nowadays, the industrial sector is progressively applying CE principles in their business strategies, and focusing on the potential positive consequences of CE eco-innovations on climate change mitigation. With the aim to promote the transition to an open-loop circular economy for automotive batteries, this study assesses and quantifies the potential environmental benefits resulting from the integration of a second-life battery-based BESS (SL-BESS) connected to an industrial machine. For this purpose, various scenarios involving the use of BESS, SL-BESS, and a standalone PV system are compared with a base case, where the machine is entirely powered by electricity from the grid. The examination of life cycle stages follows the life cycle assessment (LCA) cradle-to-grave methodology as outlined in ISO 14040:2006 and ISO 14044:2006/Amd 1:2017. Simapro® 9 is utilized as the software platform. Results demonstrate that the combination of the SL-BESS with a standalone photovoltaic (PV) system represents the optimal solution in terms of global warming potential (GWP) reduction, with a saving of up to −74.8%. However, manufacturing and end-of-life stages of PV and batteries contribute to abiotic depletion and human toxicity, resulting from the use of chemicals and the extraction of resources essential for their manufacture. Indeed, when BESS is made of new batteries, it demonstrates the most significant impacts in terms of AD at 1.22×10^{-1} kg Sb eq and human toxicity (HT) at 3.87×10^{3} kg 1,4-DB eq, primarily attributable to the manufacturing stages of both BESS and PV systems. The findings represent a significant breakthrough, highlighting the substantial capacity of incorporating SL-BESS alongside renewable energy sources to mitigate GWP resulting from industrial applications, and the criticality of repurposing decommissioned batteries from the automotive industry for secondary use.

Keywords: life cycle assessment; circular economy; second-life battery; battery energy storage system; electric vehicle; PV system

Citation: Silvestri, L.; Forcina, A.; Silvestri, C.; Arcese, G.; Falcone, D. Exploring the Environmental Benefits of an Open-Loop Circular Economy Strategy for Automotive Batteries in Industrial Applications. *Energies* **2024**, *17*, 1720. https://doi.org/10.3390/en17071720

Academic Editor: King Jet Tseng

Received: 8 March 2024
Revised: 26 March 2024
Accepted: 29 March 2024
Published: 3 April 2024

1. Introduction

The concept of circular economy (CE), a current global business trend, aims to considerably reduce waste and environmental pollution [1]. The circular economy model

entails further use of materials and products in a restorative and regenerative way, thereby extending the presence of materials, products, and components on the market [2–5]. As an example, the possibility of extending the service life of decommissioned batteries from automotive applications represents an attractive prospect [6]. In fact, the tremendous increase in the demand for batteries employed in electric vehicles (EVs) [7] raises significant issues regarding battery recycling [8] and their *reuse* or *second use* for different applications [9]. Future predictions estimate from 1.2 to 4 million tons of decommissioned lithium-ion (Li-ion) batteries being available by 2030 [10]. The dominant segments of the global battery market in 2016 consisted of lead–acid, lithium-based, and nickel-based batteries, collectively comprising 94.8% [11]. Li-ion batteries are deemed particularly suitable for future EVs owing to their superior power and energy density per unit mass [12,13]. Projections suggest that by 2030, Li-ion batteries will power 70% of hybrids, 100% of plug-in hybrids, and all electric vehicles [14,15]. Future estimations anticipate 1.2 to 4 million tons of Li-ion batteries available for recycling worldwide [10,16], with China alone projected to surpass 500 thousand tons by 2020 [17]. Consequently, the challenge of reusing, recycling, and efficiently recovering these batteries presents both a global challenge and an opportunity for the development of novel closed or open-loop circular models [18]. The literature on circular supply chain distinguishes between two distinct supply chain configurations based on product and material flows, as well as end markets. Closed-loop supply chains involve the return of products to the original manufacturer and their reprocessing for resale as perfect substitutes in the original markets. In contrast, open-loop supply chains entail the reprocessing of products and materials by entities other than the original manufacturer to serve markets different from the products' original markets [19].

In this context, the efficient recycling and reusing of decommissioned batteries is crucial for environmental protection and economic advancement. While battery recycling technologies are considered mature [20,21], the collection of decommissioned batteries remains a critical aspect from political and reverse logistic perspectives [14,22]. Governments typically set collection rate targets [14,23], and regulations such as the EU Directive 2000/53/EC [24] dictate design standards to facilitate easy recovery, reuse, and recycling of vehicle components during end-of-life stages.

The recent literature [25–28] suggests how the second-life use of decommissioned batteries from EVs is an effective and economically viable option for stationary energy storage applications in industrial settings, including the control of fluctuations in electricity supply and demand [29]. Generally, automotive batteries are typically replaced when they retain 70–80% of their original capacity [30]. Depending on the cell chemistry and specific design [9], these batteries can still be utilized in less demanding applications than automotive use [30], such as residential, commercial, and industrial uses [6]. On the other hand, while second-life batteries offer promising advantages, addressing various challenges is essential for their effective utilization [31]. One challenge associated with second-life batteries is tracing degradation, which poses a significant obstacle. Another challenge arises from safety risks during disassembly, adding to complexities beyond time and cost considerations. Additionally, assessing the safety performance of retired batteries proves challenging due to the intricate degradation processes they typically undergo.

The large-scale production and usage of automotive batteries also presents a significant concern regarding environmental impacts, as the manufacturing, application, and recycling/disposal of batteries are also sources of pollution [32]. In particular, the battery manufacturing phase involves substantial energy consumption and emissions of pollutants, prompting research to explore the possibility of repurposing end-of-life automotive batteries in battery energy storage systems (BESSs) to mitigate the environmental impacts associated with battery production and enhance battery efficiency [33]. Indeed, secondary utilization has been proven beneficial across various environmental impact categories [34]. In recent years, numerous studies have directed their attention towards assessing the environmental sustainability of battery recycling, particularly with the increasing retirement of automotive batteries [30,33,35,36]. Factors such as cell chemistry, recycling efficiency,

and the quality of recovered materials can significantly influence the environmental impact of various recycling methods [8,37,38]. A direct comparison between the recycling of lithium iron phosphate (LFP) batteries and recycling after secondary utilization in BESSs revealed that incorporating LFP secondary utilization in BESSs effectively reduces fossil fuel consumption in the life cycle [33]. Thus, if over 50% of lithium-ion batteries were repurposed, significant environmental impacts could be mitigated. Finally, from a life cycle perspective, the operational phase of batteries entails considerable environmental impacts arising from the generation of the electricity required for their recharging [39], which vary depending on the carbon footprint characteristic of the electricity mix being utilized. For example, in Europe, this mix ranges from 56 gCO_2eq/kWh in France to 692 gCO_2eq/kWh in Poland [40]. For this reason, numerous studies are investigating the integration of BESS with renewable energy generators, such as wind or photovoltaics (PVs) [6,41].

Based on the findings presented in the aforementioned research, repurposing Li-ion batteries from EVs for BESS represents a feasible pathway. The majority of the studies related to environmental impact assessment concentrate on aspects related to the manufacturing and recycling processes of Li-ion batteries. However, these studies do not sufficiently focus on the criticality of the use phase of BESS in terms of environmental impacts, whether they involve new batteries or their second life. These impacts are significantly influenced by national electricity mixes, highlighting the necessity for integration with green technologies for power supply to make BESSs significantly more sustainable throughout their life cycle.

This study aims to investigate the extent to which the implementation of an open-loop circular economy strategy for second-life batteries can improve sustainability of industrial applications. To this end, the authors conduct a cradle-to-grave life cycle assessment (LCA) to assess and compare different settings of BESS made of new or second-life batteries (SL-BESS) combined with a standalone PV system serving a ball mill machine in a ceramic manufacturing plant.

The LCA is widely recognized as one of the most commonly used tools for analyzing and comparing the environmental loads of energy systems [8,42]. It enables the allocation of environmental impacts to each stage of the life cycle, serving as a valuable decision support tool for identifying less impactful energy scenarios. This study also identifies and discusses potential hotspots, characterized by activities or elementary flows that make a significant contribution to the overall environmental impact. Finally, the recycling of Li-ion batteries is an emerging area that is likely to undergo significant changes as the process evolves to address various challenges [43]. To this end, this study provides a useful detailed inventory for the recycling stage, focusing on hydrometallurgy, which is considered one of the best routes for the recovery of the metals of interest.

The authors believe that the awareness of the potential environmental gains derived from the use of renewable energy-based power sources integrated with BESSs made of decommissioned batteries will lead companies towards green technology investments and mitigation of emissions.

This paper is organized as follows: Section 2, "Materials and Methods", describes the methodology utilized for the LCA study, including the goal and scope, the modeling of comparative scenarios, the technical parameters of the considered system, and a detailed description of the manufacturing, use phase, and end-of-life stages. Section 3, "Results and Discussion", presents a comparative analysis among the scenarios, environmental hotspots, and discussions. Finally, the concluding remarks, along with proposals for further research directions, are provided in Section 4 "Conclusions".

2. Materials and Methods

In this study, a comparative LCA analysis related to the use of a BESS integrated with a standalone PV system serving a ball mill machine in a ceramic manufacturing plant is performed.

The aim is to evaluate how the environmental impact categories can be reduced, replacing the direct grid supply with electricity stored in a BESS or a second-life BESS (SL-BESS).

2.1. Phases of Life Cycle Assessment

The research adopts the LCA methodology, which entails a comprehensive analysis of material and energy flows and their resultant environmental impacts across the entire lifespan of a product or process, spanning from raw material extraction to product disposal or end of service life. The methodological framework and standards for LCA are delineated by ISO 14040-14044 and the Joint Research Centre standards, supplemented by additional guidelines according to various product categories and global regions, such as those offered by the International Reference Life Cycle Data (ILCD) system. The LCA methodology was applied in several recent studies related to storage of energy [42,44,45] and electric powertrains [46,47], and to understand the sustainability impacts of CE strategies [48,49]. The LCA standards employ a four-step approach, comprising (1) defining the goal and scope, (2) conducting inventory assessment, (3) performing impact assessment, and (4) interpreting the results.

According to ISO 14040-14044 standards [50,51], the LCA employs a four-step approach (Figure 1), comprising (1) defining the goal and scope, (2) conducting inventory assessment, (3) performing impact assessment, and (4) interpreting the results, as follows:

- **Step 1**. Goal and scope definition. This step identifies the total objectives and gives a picture of the system in terms of system boundary and functional unit (FU);
- **Step 2**. Life cycle inventory analysis (LCI). This step includes the data collection on raw materials and energy consumption, environmental emissions, and waste generation;
- **Step 3**. Life cycle impact assessment (LCIA). This phase results in the classification of the environmental impacts of all processes previously collected and modeled in the LCI phase and transforms them into environmental themes such as global warming or human health.
- **Step 4**. Interpretation. This last step allows the LCIA results to be comparable and comprehensible.

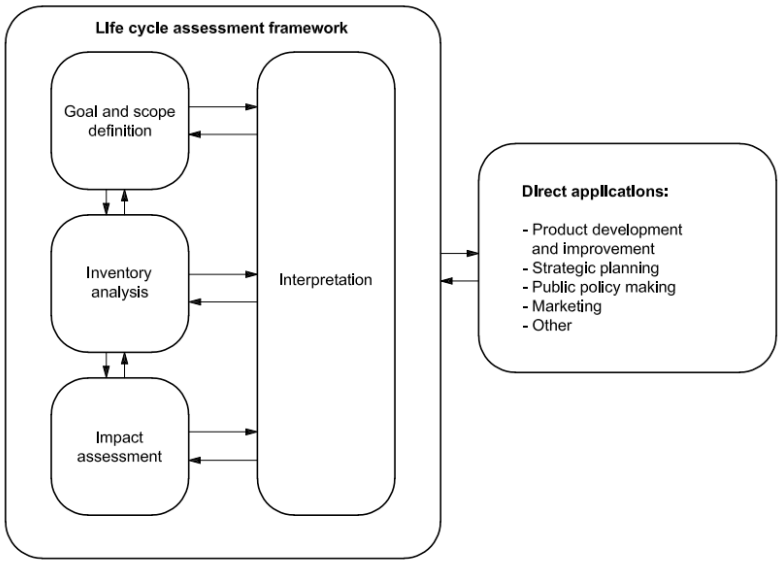

Figure 1. LCA stages according to ISO 14040 and ILCD guidelines. Source: [50].

2.2. Life Cycle Assessment: Goal and Scope

The LCA conducted in this study serves to identify the best solution for the integration of a BESS integrated with a standalone PV system serving a ball mill machine in a ceramic manufacturing plant. To this end, four different scenarios are compared to a base case

where neither a PV system nor a BESS are considered with the ball mill directly connected to the national grid.

In particular, this investigation is conducted within the framework of a ceramic production facility encompassing grinding, casting, drying, glazing, firing, and packing phases of its industrial process. The grinding operation is carried out by a ball mill machine, standing out as the primary consumer of electricity within the manufacturing process [28]. The ball mill can be served according to different scenarios described as follows:

- **Base Case**: the ball mill machine is entirely served by the grid supply;
- **Scenario 1**: the ball mill machine is served by a BESS made of new batteries connected to the grid;
- **Scenario 2**: the ball mill machine is served by a BESS made of new batteries connected to a standalone PV system;
- **Scenario 3**: the ball mill machine is served by a SL-BESS made of decommissioned automotive batteries connected to the grid;
- **Scenario 4**: the ball mill machine is served by a SL-BESS made of decommissioned automotive batteries connected to a standalone PV system.

The scenarios differ in technical parameters and energy load management strategies for the considered industrial load, as indicated in Section 2.3. All scenarios consider the same lifespan and energy efficiencies of the BESS, SL-BESS, and PV system. Furthermore, the available decommissioned batteries considered in this study are assumed to be homogeneous and characterized by Li-ion batteries based on the same chemistry and residual capacity as specified in Sections 2.3.1 and 2.3.3.

The comparative scenarios are simulated using the standardized *cradle-to-grave* LCA methodology outlined in ISO 14040/44 [50,51]. The selected impact categories under examination are summarized in Table 1, utilizing the CML-IA midpoint-oriented method developed by the Center of Environmental Science of Leiden University (CML) [52,53] for the LCIA phase. The CML approach is selected based on its broad acceptance and prevalent application across various LCA automotive analyses. Given its consistent use in comparable research, it produces robust outcomes for mid-point potential impacts, facilitating effective comparisons. Among environmental impact categories, abiotic depletion (AD), human toxicity (HT), and global warming potential (GWP) are selected as the most representative indicators for comparing results [8].

The quantification of environmental emissions is conducted in relation to the functional unit (FU) defined as "*One year of operation of a ball mill*". The system boundary is illustrated in Figure 2. Main activities are grouped into *foreground processes*, which include core processes of the manufacturing, use, and recycling phase of the BESS and the PV system, and *background processes*, which are indirectly involved in the BESS and PV system cradle-to-grave chain, such as water supply, thermal energy, electricity, and raw materials transport. The cut-off criteria are established to neglect processes whose contribution accounts for less than 1% of the overall environmental burden. The LCA is performed by using the software *SimaPro*® [54] and data available in the literature and records included in the Ecoinvent 3.5 database [55]. Finally, the LCIA is carried out through the CML-IA midpoint-oriented method developed by the Center of Environmental Science of Leiden University (CML) [52,53].

Table 1. Environmental impact categories and category indicators associated to the CML method (baseline). Source: [56].

Impact Category Group	Name of the Impact Category	Acronym	Unit of Measurement
Depletion of abiotic resources	Depletion of abiotic resources (elements, ultimate reserves)	AD	kg Sb eq.
	Depletion of abiotic resources (fossil fuels)	AD(ff)	MJ

Table 1. *Cont.*

Impact Category Group	Name of the Impact Category	Acronym	Unit of Measurement
Climate change	Climate change (global warming potential)	GWP	kg CO_2 eq.
Ozone layer depletion	Ozone layer depletion	ODP	kg CFC-11 eq.
Human toxicity	Human toxicity	HT	kg 1,4-DB eq.
Ecotoxicity	Fresh water aquatic ecotoxicity	FWAE	kg 1,4-DB eq.
	Marine aquatic ecotoxicity	MAE	kg 1,4-DB eq.
	Terrestrial ecotoxicity	TE	kg 1,4-DB eq.
Photochemical oxidation	Photochemical oxidation	POC	kg C_2H_4 eq.
Acidification	Acidification potential	A	kg SO_2 eq.
Eutrophication	Eutrophication	E	kg PO_4 eq.

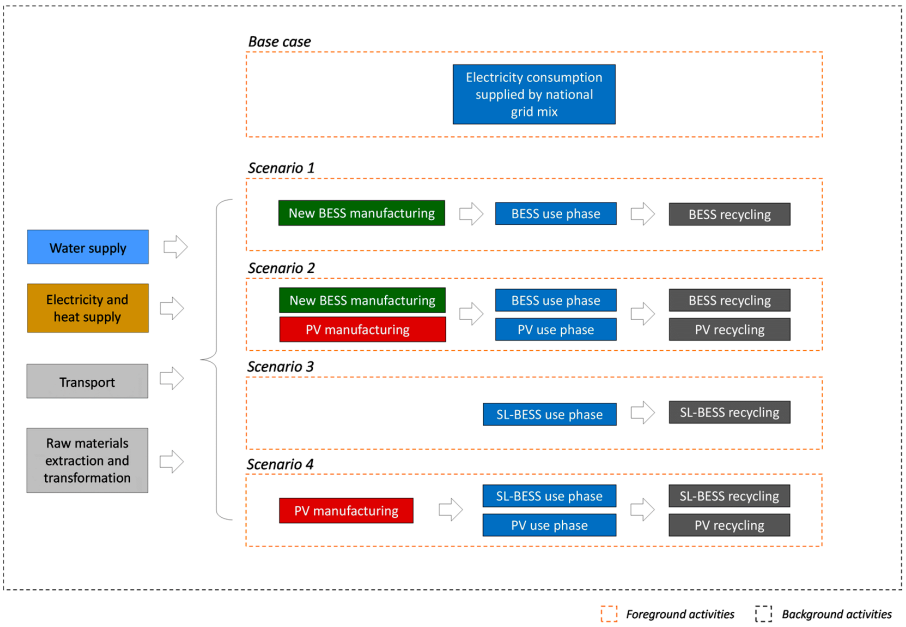

Figure 2. System boundary.

2.3. Data Collection and Key Assumptions

In this paragraph, data collection and key assumptions are presented.

2.3.1. Manufacturing and Recycling of BESS

The most common cathode chemistries for BEVs include lithium manganese oxide (LMO), lithium nickel manganese cobalt oxide (NMC), lithium iron phosphate (LFP), and lithium nickel cobalt aluminum (NCA). Both lithium and cobalt are deemed critical materials by major global economies like the U.S., China, and Europe due to their potential geopolitical supply risks in the ongoing transition to renewable energy. Scholars highlight cobalt as the most valuable component of present BEV traction batteries. Consequently, there is a growing focus on cobalt-free chemistries to enhance their performance metrics such as specific capacity, volumetric energy density, and lifespan. For instance, current commercial LFP batteries are recognized for their safety and durability despite offering a relatively modest specific energy range of 80–150 Wh/kg compared with other Li-ion chemistries. If the market moves away from cathodes that contain cobalt, there is a possibility that LFP batteries could become dominant in the market in the near future, as

evidenced by Tesla's plan to adopt a new generation of LFP technology in Model 3 for the Chinese market [57]. For these reasons, the LFP chemistry has been chosen for the BESS examined in this study. The LFP battery consists of a $LiFePO_4$ cathode and a graphite anode. The material inventory has been obtained from the literature and Ecoinvent [55,58]. The battery production involves the following three main steps: electrode preparation, cell manufacture, and battery assembly. The paste used for both electrodes is directly prepared in the factory when the battery is assembled, where a coating machine applies a slight coat of 200–250 μm on the sides of the electrode substrates. The fine sludge is then dried and flattened. Subsequently, the separator and the electrodes are packed together and wound-up inside the cell container. Cells are joined with the electrolyte and closed. The cells are always produced completely discharged, and all the ions are located in the lithium battery cathode. Subsequently, the cells are tested through a specific number of charge–discharge cycles and standardized conformity tests. The cells are arranged in modules in the final battery pack. The overall energy consumption has been estimated to be 55.6 MJ per kg of battery, divided into 28.6 MJ thermal energy and 27 MJ of electricity. Thermal energy is derived from natural gas. Furthermore, the water required is 65.1 L per kg of battery. Finally, the transportation of raw materials and final products have been modeled according to the literature [58].

The selected method for the recycling of the LFP battery is the emerging ultra-high temperature (UHT) method developed by Umicore company [59]. The recycling steps include the battery collection, transportation, and a pretreatment phase, which consists of disassembling the battery pack by hand. In this way, it is possible to separate some components and valuable parts for the next processes. Subsequently, modules are crushed in an inert atmosphere to reduce the risk of fire. A four-shaft rotary shear is employed for module crushing. The conversion phase consists of a UHT smelting step [60], which demands a total thermal energy of 5.26 MJ per kg of decommissioned batteries. The UHT furnace is fueled by coke and a slag-forming agent, such as limestone, sand, or slag. As a result, a lithium-rich flue dust is obtained and subsequently treated by leaching treatment. Finally, chemical precipitation, oxidation, and a sintering phase are conducted through the addition of Na_2CO_3, H_2O_2, and Li_2CO_3. The total electricity required for the recycling phase is 75 MJ per kg of decommissioned batteries. An extraction of raw materials inventory for both manufacturing and recycling is shown in Table 2.

Table 2. Example data extracted from the main inventory dedicated to input materials into the system. The values refer to the considered FU.

PV Panel Manuf.		**PV Panel O&M**		**PV Panel End-of-Life**		**BESS Manuf.**		**BESS End-of-Life**	
Glass (kg)	1096.9	Water demin. (kg)	2.41×10^{0}	Tap water (kg)	453.0	Water, decarb. (l)	3.80×10^{2}	Water (l)	9.75×10^{2}
Polymer (kg)	146.3	Hydraulic oil (kg)	2.05×10^{-2}	Nitric acid (kg)	10.4	Deionized water (kg)	2.50×10^{2}	Coke (kg)	3.93×10^{3}
Aluminum (kg)	117.0	Polyester (kg)	1.36×10^{-3}	Lime, hydrated (kg)	53.4	Positive electrode paste (kg)	6.25×10^{0}	H_2SO_4 (kg)	1.11×10^{4}
Silicon (kg)	73.1	Co-polymer plastic (kg)	9.10×10^{-4}			Iron sulphate ($FeSO_4$) (kg)	5.44×10^{0}	Li_2CO_3 (kg)	1.90×10^{3}
Copper (kg)	14.6	Lubricating oil (kg)	5.69×10^{-4}			Cell container, tab and terminals (kg)	2.00×10^{-1}	H_2O_2 (kg)	1.98×10^{3}
		Polyurethane (kg)	2.05×10^{-4}			Module and battery packaging (kg)	1.70×10^{-1}	Limestone (kg)	3.32×10^{4}
		Silica gel (kg)	2.05×10^{-4}			Phosphoric acid (H_3PO_4) (kg)	3.53×10^{0}		
		Stainless steel (kg)	1.59×10^{-4}			Electrolyte for li-ion battery (kg)	1.20×10^{-1}		
		Glass fiber (kg)	1.59×10^{-4}						
		Poly carbonate (kg)	6.82×10^{-5}						
		Poly amide (kg)	2.27×10^{-5}						

2.3.2. Manufacturing and Recycling of PV System

The PV system is assumed to be made of single module PS Alps-X monocrystalline 240 W (tilt angle of around 35°), which has a power output of 240 W, weighs 19.5 kg, and covers an area of 1.64 m^2. The number of series and parallel modules in the PV array is 15 and 5 modules, respectively. The overall power of the PV system is 18 kWp, allowing a BESS charging C/3 rate. The manufacturing and recycling of the PV system is modeled according to the literature and Ecoinvent [55]. A common crystalline silicon PV module is made of approximately three-quarters of the total weight of module surface made with glass, 10% polymer that constitutes the encapsulant and backsheet foil, 8% aluminum used for making the frame, 5% silicon thin film solar cells, 1% copper used for the interconnectors, and less than 0.1% silver for the contact lines; other metals employed in lower percentages are mainly tin and lead. The main raw material inputs required for the manufacturing stage are summarized in Table 2.

The end-of-life stage of PV system parts includes the following steps: the system decommissioning and component transportation to the recycling plant, the shredding and separation of components, and, finally, the disposal of the unrecyclable parts. For decommissioning, the recycling plant is assumed to be located 100 km distant from the PV system location. The energy required for the shredding and separation stages is 0.1 MJ/kg and 0.24 MJ/kg, respectively. It is assumed that the separation step did not require parts with homogeneous material composition. The total electricity and diesel fuel required for recycling activities is 0.11355 kWh and 0.00114 L per ton of PV panel, respectively.

2.3.3. Use Phase

The use phase of the BESS and PV system is modeled according to data already presented by the authors in previous publications [28,61]. The BESS serves a ball mill machine used in a ceramic factory located in the industrial district of Civita Castellana in the Province of Viterbo (Central Italy). The monthly energy output for the PV system is simulated using the European Photovoltaic Geographical Information System (PVGIS) [62] simulation tool (Figure 3), according to the latitude of the considered place and installed peak PV power.

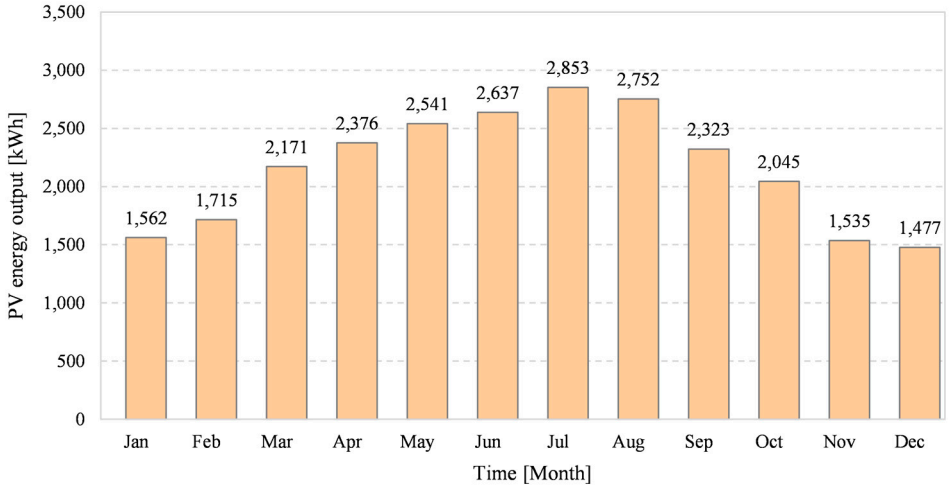

Figure 3. Simulated monthly energy output for the PV system. Source: (C) PVGIS, 2021.

The first step of ceramic manufacturing is the preparation and mixing of raw materials, mainly made with the use of the ball mill machine for the grinding procedure. In this phase, raw materials are mixed with water in appropriate proportions and particles, reducing up to a 5 mm diameter.

The ball mill machine is a grinder extensively utilized in industries such as cement, ores, and ceramics [63], and comprises a hollow cylindrical rotating shell partially filled

with steel spheres (grinding balls). This shell rotates around its axis at a speed enabling the cascading effect of the spheres' fall [64]. Within the ball mill, input materials undergo grinding facilitated by the impact of grinding balls through the following three primary breakage mechanisms: impact or compression, chipping or attrition, and abrasion [65].

As aforementioned, the ball milling process generally accounts for the highest electricity consumption within the manufacturing processes [66]. Operating continuously throughout extended periods within the working day [67], its power consumption can vary from less than 80 kW for ceramic processes [68] to 3.9 MW for gold ore processing [69]. The considered ball mill has a nominal power of 160 kW and the daily load profile of the ball mill is derived from Ref. [67].

For all the scenarios, the BESS supplies the electrical power to the ball mill for a timing of about 2.91 h, during the national on-peak time period. Indeed, the choice of this time window guarantees an optimal solution for the sizing of the BESS system, obtaining both environmental and economic advantages [27,28]. The assumed overall electricity consumption for the ball mill is approximately 88 kWh per day, with a peak current of 134 A at low voltage distribution (Figure 2); the nominal power is 160 kW. For all the scenarios, the average European (EU-27) electricity generation mix is modeled in Ecoinvent.

BESS is made of a total of 22,000 cells in series-parallel configuration and sorted into about 54 modules [28]. The BESS capacity is 200 kWh. When second-life batteries are considered (Scenario 3 and Scenario 4), the remaining capacity of cells is assumed equal to 80% of the original one. Finally, the lifespan of the second-life BESS and PV system is assumed to be 10 years [70], with a depth-of-discharge of about 30% to 40%. On the other hand, the lifespan of the PV system is assumed to be 20 years [71]. The daily power consumption of the ball mill is shown in Figure 4, while the annual consumption is shown in Table 3.

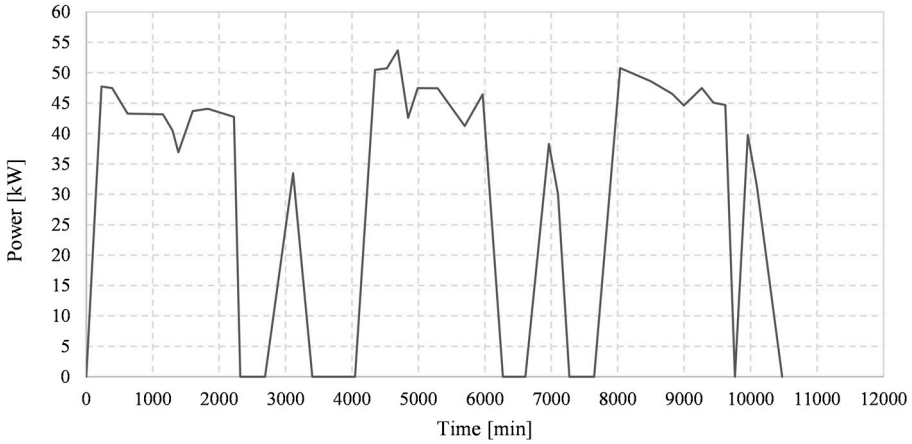

Figure 4. The assumed daily power consumption of the ball mill on a typical workday. Source: [67].

Table 3. Electricity powering the ball mill originated from the electric grid.

	Base Case	Scenario 1	Scenario 2	Scenario 3	Scenario 4
Electricity from grid [kWh/y]	32,120	32,120	6135	32,120	6135

A maintenance stage has been designed for the PV system, taking into account materials substitutions, such as hydraulic and bearing oils and oil filters and activities of cleaning lenses and general inspections [72] (see Table 2). On the other hand, the maintenance stage for BESS and SL-BESS has not been included in accordance with the cut-off criteria outlined in Section 2.2.

3. Results and Discussion

Results obtained through the use of the CML-IA are summarized in Tables 4–8. Table 4 shows the environmental impact indicators of the base case scenario, where the ball mill machine is solely and directly powered by the national electric grid. According to the considered system boundary (Figure 2), the environmental impacts for the base case are only those associated with the electricity generation mix, which are influenced by diverse factors, including the mix's composition. Indeed, fossil-fuel-based power generation typically demonstrates a more significant environmental footprint compared with renewable energy sources. AD correlates with the utilization of materials within the energy generation mix, encompassing metals and minerals employed in power plant construction or fossil fuel extraction. Renewable energy sources also necessitate materials for infrastructure, although in smaller quantities, thereby still contributing to the depletion of abiotic resources. AD(ff) corresponds to the consumption of fossil fuels within the energy generation composition, particularly coal, oil, and natural gas. The GWP reflects the contribution of power generation to climate change through greenhouse gases (GHGs). The generation mix that is heavily reliant on fossil fuels, particularly coal and oil, will have a higher GWP due to the significant emissions of carbon dioxide during combustion. The ODP measures the potential impact on the ozone layer, and power generation can indirectly contribute to this indicator due to certain industrial processes associated with power generation. These processes involve the use of refrigerants or the production of industrial chemicals, which may contribute to emissions of ozone-depleting substances like chlorofluorocarbons (CFCs). HT is associated with emissions of toxic substances from power generation activities, particularly from combustion processes. This includes pollutants like heavy metals, which can pose risks to human health through air and water contamination. FWAE measures the potential impact on freshwater aquatic ecosystems, which is likely caused by the discharge of pollutants from power plants into rivers, lakes, and other freshwater environments. This could include heavy metals, chemicals, and thermal pollution. MAE reflects the potential impact on marine aquatic ecosystems, which may result from the discharge of pollutants into coastal waters or rivers that flow into oceans. Renewable energy sources may have indirect impacts on marine ecosystems, such as offshore wind farms affecting marine habitats, but typically have lower direct emissions compared with fossil fuels. The TE indicator is associated with the release of toxic substances into soil and land, which can occur through various pathways such as coal ash disposal, landfills, or accidental spills from power plant operations. POC is linked to emissions of volatile organic compounds (VOCs) and nitrogen oxides (NOxs) from combustion processes in power plants. These pollutants contribute to the formation of ground-level ozone, which can harm human health and ecosystems. The A indicator refers to the acidification potential resulting from sulfur dioxide (SO_2) emissions, primarily from the combustion of sulfur-containing fossil fuels like coal and oil. Indeed, power plants emitting high levels of SO_2 contribute to acid rain and acidification of soil and water bodies. Finally, power plants can indirectly contribute to eutrophication (E) through the discharge of nutrient-rich wastewater or cooling water into water bodies. This can lead to excessive algae growth and oxygen depletion, impacting aquatic ecosystems. While renewable energy sources have lower direct emissions, their impacts on eutrophication may include land use changes or habitat disruption during construction.

Table 5 summarizes environmental impact indicators for Scenario 1, when the ball mill machine is served by a BESS made of new batteries connected to the grid. As can be seen, the indicators related to the use phase are the same as Scenario 1, being the ball mill machine and the BESS powered by the same electricity mix. Scenario 2 also accounts for the manufacturing and the end-of-life stages for a BESS made of new batteries. The manufacturing stage is responsible for a significant fraction of the overall environmental impact. Indeed, resource extraction processes such as lithium brine mining and hard rock mining require significant amounts of water, resulting in water scarcity issues in arid regions where lithium deposits are commonly found. Additionally, mining activities can interfere with ecosystems. Furthermore, lithium-based BESS manufacturing involves

several energy-intensive steps, including processing raw materials, synthesizing electrode materials, and assembling battery cells (Section 2.3.1). Much of this energy comes from fossil fuel sources, leading to GHGs and contributing to climate change. The battery production requires various chemicals, such as solvents, electrolytes, and binders (Table 2). Finally, the transportation of raw materials, components, and finished batteries involves energy consumption and emissions, contributing to air pollution and GHGs.

Generally, the manufacturing stage involves higher environmental impacts than the end-of-life stage; in fact, it demands extensive energy, raw material extraction, and chemical processes, contributing to its larger environmental footprint. In contrast, the end-of-life stage involves managing smaller volumes of waste compared with the extensive inputs and outputs of the manufacturing process. In particular, GWP is 1.22×10^3 kg CO_2 eq. per year and is an order of magnitude larger in manufacturing compared with end-of-life, while AD and HT are 1.20×10^{-1} kg Sb eq. and 3.38×10^3 kg 1,4-DB eq., respectively, and three and two orders of magnitude higher than end-of-life, respectively.

Table 4. Life cycle impact assessment (LCIA) results for the base case (CML-IA method). Values refer to the functional unit.

		Use Phase (Ball Mill)
AD	kg Sb eq	1.07×10^{-3}
AD(ff)	MJ	1.69×10^{5}
GWP	kg CO_2 eq	1.51×10^{4}
ODP	kg CFC-11 eq	9.58×10^{-4}
HT	kg 1,4-DB eq	4.04×10^{2}
FWAE	kg 1,4-DB eq	2.42×10^{1}
MAE	kg 1,4-DB eq	1.45×10^{6}
TE	kg 1,4-DB eq	7.98×10^{0}
POC	kg C_2H_4 eq	3.39×10^{0}
A	kg SO_2 eq	6.15×10^{1}
E	kg PO_4 eq	3.46×10^{0}

Table 5. Life cycle impact assessment (LCIA) results for Scenario 1 (CML-IA method). Values refer to the functional unit.

S1		**Manuf. (New-BESS)**	**Use Phase (Ball Mill)**	**End-of-Life (New-BESS)**	**Total**
AD	kg Sb eq	1.20×10^{-1}	1.07×10^{-3}	4.66×10^{-4}	1.22×10^{-1}
AD(ff)	MJ	1.21×10^{4}	1.69×10^{5}	1.68×10^{3}	1.83×10^{5}
GWP	kg CO_2 eq	1.22×10^{3}	1.51×10^{4}	1.34×10^{2}	1.64×10^{4}
ODP	kg CFC-11 eq	8.13×10^{-3}	9.58×10^{-4}	1.05×10^{-5}	9.10×10^{-3}
HT	kg 1,4-DB eq	3.38×10^{3}	4.04×10^{2}	8.10×10^{1}	3.87×10^{3}
FWAE	kg 1,4-DB eq	1.66×10^{3}	2.42×10^{1}	5.52×10^{1}	1.74×10^{3}
MAE	kg 1,4-DB eq	5.58×10^{6}	1.45×10^{6}	2.26×10^{5}	7.25×10^{6}
TE	kg 1,4-DB eq	5.62×10^{0}	7.98×10^{0}	1.90×10^{-1}	1.38×10^{1}
POC	kg C_2H_4 eq	3.79×10^{-1}	3.39×10^{0}	1.23×10^{-1}	3.89×10^{0}
A	kg SO_2 eq	7.56×10^{0}	6.15×10^{1}	9.95×10^{-1}	7.01×10^{1}
E	kg PO_4 eq	6.20×10^{0}	3.46×10^{0}	2.41×10^{-1}	9.90×10^{0}

Scenario 2 involves the utilization of a ball mill machine powered by a BESS comprising newly manufactured batteries that are connected to an independent PV system. Table 6 highlights environmental impact indicators for all the involved stages, which are the manufacturing of BESS and PV; the electricity consumed during the use phase of the ball mill and the PV O&M; and end-of-life stages for both BESS and PV. Compared with Scenario 1 and the base case, the use phase of the ball mill is significantly lower. This is attributed to the source of the consumed electricity, which is partially provided by the PV system and associated with significantly lower emissions. In particular, emissions from the PV system arise only from the PV O&M processes. As a result, total GWP is 5.03×10^3 kg CO_2 eq. However, total AD and HT are 1.66×10^{-1} kg Sb eq. and 4.09×10^3 kg 1,4-DB eq., respectively. Indeed, significant energy and raw material inputs are required to produce PV panels (Table 2). This includes the extraction of materials such as silicon, glass, metals, and other components, which can contribute to AD and GHGs. Additionally, the manufacturing process generally involves the use of chemicals and substances that can pose risks to human health (HT). Finally, the end-of-life stage involves environmental impacts due to the complex composition of PV panels, including metals, glass, and potentially hazardous materials. Recycling PV panels involves disassembly, sorting, and processing of different materials. This process consumes energy and resources, such as electricity and water, especially during the extraction of valuable components like silicon and metals.

Table 6. Life cycle impact assessment (LCIA) results for Scenario 2 (CML-IA method). Values refer to the functional unit.

S2		Manuf. (New-BESS)	Manuf. (PV)	Use Phase (Ball Mill)	Use Phase (PV O&M)	End-of-Life (New-BESS)	End-of-Life (PV)	Total
AD	kg Sb eq	1.20×10^{-1}	4.50×10^{-2}	2.05×10^{-4}	4.17×10^{-6}	4.66×10^{-4}	6.00×10^{-6}	1.66×10^{-1}
AD(ff)	MJ	1.21×10^4	8.62×10^3	3.23×10^4	1.18×10^2	1.68×10^3	2.14×10^1	5.49×10^4
GWP	kg CO_2 eq	1.22×10^3	7.83×10^2	2.88×10^3	3.37×10^0	1.34×10^2	4.67×10^0	5.03×10^3
ODP	kg CFC-11 eq	8.13×10^{-3}	4.76×10^{-5}	1.83×10^{-4}	9.09×10^{-8}	1.05×10^{-5}	1.91×10^{-7}	8.38×10^{-3}
HT	kg 1,4-DB eq	3.38×10^3	5.47×10^2	7.72×10^1	7.06×10^0	8.10×10^1	8.44×10^{-1}	4.09×10^3
FWAE	kg 1,4-DB eq	1.66×10^3	4.38×10^2	4.61×10^0	2.39×10^0	5.52×10^1	5.72×10^{-1}	2.16×10^3
MAE	kg 1,4-DB eq	5.58×10^6	1.71×10^6	2.77×10^5	9.03×10^3	2.26×10^5	1.28×10^3	7.80×10^6
TE	kg 1,4-DB eq	5.62×10^0	1.39×10^0	1.52×10^0	3.88×10^{-3}	1.90×10^{-1}	8.10×10^{-3}	8.74×10^0
POC	kg C_2H_4 eq	3.79×10^{-1}	1.83×10^{-1}	6.48×10^{-1}	2.20×10^{-3}	1.23×10^{-1}	6.06×10^{-4}	1.34×10^0
A	kg SO_2 eq	7.56×10^0	3.98×10^0	1.17×10^1	2.68×10^{-2}	9.95×10^{-1}	1.01×10^{-2}	2.43×10^1
E	kg PO_4 eq	6.20×10^0	1.97×10^0	6.62×10^{-1}	2.49×10^{-3}	2.41×10^{-1}	3.38×10^{-3}	9.07×10^0

Scenario 3 introduces the use of BESS made of decommissioned automotive batteries connected to the grid. In this scenario, the utilization of batteries sourced from previous applications allows for the exclusion of BESS manufacturing in the calculation of environmental impacts. The relative CML-IA indicators are shown in Table 7. As previously mentioned, the end-of-life process of BESS is assumed to be the same for both used batteries and new batteries. Therefore, the impacts of the end-of-life phase remain consistent with those of Scenario 1 and Scenario 2. The total GWP, AD, and HT are 1.52×10^4 kg CO_2 eq., 1.54×10^{-3} kg Sb eq., and 4.85×10^2 kg 1,4-DB eq., respectively.

Finally, in Scenario 4 the ball mill machine is served by a SL-BESS made of decommissioned automotive batteries connected to a standalone PV system. In this case, the only manufacturing stage is that of the PV system. The use phase encompasses environmental impacts arising from the electricity consumption of the ball mill (Table 8) and the O&M of the PV. Lastly, both the PV panels and the BESS will contribute to the end-of-life environmental impacts. The total GWP, AD, and HT are 3.80×10^3 kg CO_2 eq., 1.54×10^{-3} kg Sb eq., and 4.85×10^2 kg 1,4-DB eq., respectively.

Table 7. Life cycle impact assessment (LCIA) results for Scenario 3 (CML-IA method). Values refer to the functional unit.

		Use Phase (Ball Mill)	End-of-Life (SL-BESS)	Total
AD	kg Sb eq	1.07×10^{-3}	4.66×10^{-4}	1.54×10^{-3}
AD(ff)	MJ	1.69×10^5	1.68×10^3	1.71×10^5
GWP	kg CO_2 eq	1.51×10^4	1.34×10^2	1.52×10^4
ODP	kg CFC-11 eq	9.58×10^{-4}	1.05×10^{-5}	9.68×10^{-4}
HT	kg 1,4-DB eq	4.04×10^2	8.10×10^1	4.85×10^2
FWAE	kg 1,4-DB eq	2.42×10^1	5.52×10^1	7.93×10^1
MAE	kg 1,4-DB eq	1.45×10^6	2.26×10^5	1.68×10^6
TE	kg 1,4-DB eq	7.98×10^0	1.90×10^{-1}	8.17×10^0
POC	kg C_2H_4 eq	3.39×10^0	1.23×10^{-1}	3.52×10^0
A	kg SO_2 eq	6.15×10^1	9.95×10^{-1}	6.25×10^1
E	kg PO_4 eq	3.46×10^0	2.41×10^{-1}	3.71×10^0

Table 8. Life cycle impact assessment (LCIA) results for Scenario 4 (CML-IA method). Values refer to the functional unit.

		Manuf. (PV)	Use Phase (Ball Mill)	Use Phase (PV O&M)	End-of-Life (SL-BESS)	End-of-Life (PV)	Total
AD	kg Sb eq	4.50×10^{-2}	2.05×10^{-4}	4.17×10^{-6}	4.66×10^{-4}	6.00×10^{-6}	4.57×10^{-2}
AD(ff)	MJ	8.62×10^3	3.23×10^4	118.1996	1.68×10^3	2.14×10^1	4.27×10^4
GWP	kg CO_2 eq	7.83×10^2	2.88×10^3	3.365216	1.34×10^2	4.67×10^0	3.80×10^3
ODP	kg CFC-11 eq	4.76×10^{-5}	1.83×10^{-4}	9.09×10^{-8}	1.05×10^{-5}	1.91×10^{-7}	2.41×10^{-4}
HT	kg 1,4-DB eq	5.47×10^2	7.72×10^1	7.059923	8.10×10^1	8.44×10^{-1}	7.13×10^2
FWAE	kg 1,4-DB eq	4.38×10^2	4.61×10^0	2.387827	5.52×10^1	5.72×10^{-1}	5.01×10^2
MAE	kg 1,4-DB eq	1.71×10^6	2.77×10^5	9034.775	2.26×10^5	1.28×10^3	2.23×10^6
TE	kg 1,4-DB eq	1.39×10^0	1.52×10^0	0.003878	1.90×10^{-1}	8.10×10^{-3}	3.12×10^0
POC	kg C_2H_4 eq	1.83×10^{-1}	6.48×10^{-1}	0.002205	1.23×10^{-1}	6.06×10^{-4}	9.57×10^{-1}
A	kg SO_2 eq	3.98×10^0	1.17×10^1	0.026822	9.95×10^{-1}	1.01×10^{-2}	1.68×10^1
E	kg PO_4 eq	1.97×10^0		0.002486	2.41×10^{-1}	3.38×10^{-3}	2.21×10^0

The comparison among scenarios for all CML-IA indicators is depicted in Figure 5 in terms of relative percentage. Notably, Scenario 2 exhibits the highest values across various impact indicators, particularly in AD, with values reaching 49.38% and 9%. Conversely, Scenario 4 consistently displays the lowest values across most categories, indicating comparatively reduced environmental impacts. Noteworthy variations are observed in ozone depletion potential (ODP) and freshwater aquatic ecotoxicity (FWAE), where Scenario 1 and Scenario 3, respectively, demonstrate pronounced impacts.

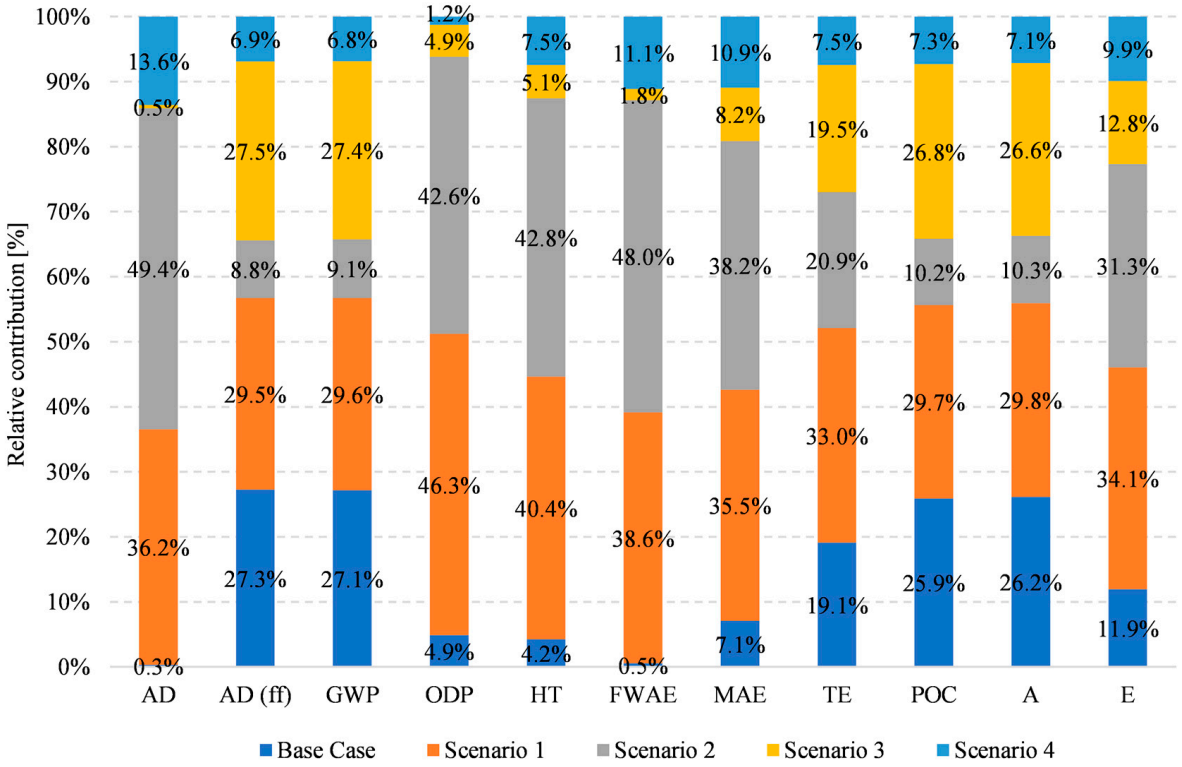

Figure 5. Life cycle impact assessment (LCIA) relative contributions of scenarios for each impact category (CML-IA method).

Figure 6 shows the comparative analysis among the scenarios for the GWP, AD, and HT indicators. Scenario 1 emerges as the most significant contributor to GWP, with a notably elevated value of 1.64×10^4 kg CO_2 eq. Furthermore, Scenario 1 shows an increase in GWP by 8.61% with respect to the base case and presents the lowest impacts across the AD and HT indicators. On the other hand, Scenario 2 demonstrates the most substantial impact on both AD and HT, with values of 1.66×10^{-1} kg Sb eq and 4.09×10^3 kg 1,4-DB eq, respectively. In particular, Scenario 2 notably exhibits a substantial decrease in GWP, registering a reduction of approximately 66.52% relative to the base case. On the other hand, it exhibits the highest impacts in terms of AD and HT, primarily due to the manufacturing stages of BESS and PV. Moreover, Scenario 3 displays a marginal increase in GWP by approximately 0.66%, with moderate impacts on both AD and HT, registering rises of 44.86% and 20.05%, respectively. Finally, Scenario 4 similarly shows a significant decrease in GWP, reaching around −74.82%. Thus, as it is possible to note, the manufacturing stage of PV and batteries significantly contributes to abiotic depletion via the extraction of metals and minerals essential for their manufacture, entailing intensive mining activities and causing habitat degradation and soil erosion. Moreover, the transportation of materials and energy-intensive processes such as smelting are reliant on fossil fuels, amplifying the depletion of finite energy resources and GHGs. Furthermore, the disposal of chemicals and solvents for cleaning, coating, and other purposes during production leads to soil and water contamination, contributing to AD by disrupting natural ecosystems and contaminating resources. On the other hand, emissions and releases from manufacturing facilities can contribute to HT, posing risks to human health through pollutants and water contamination.

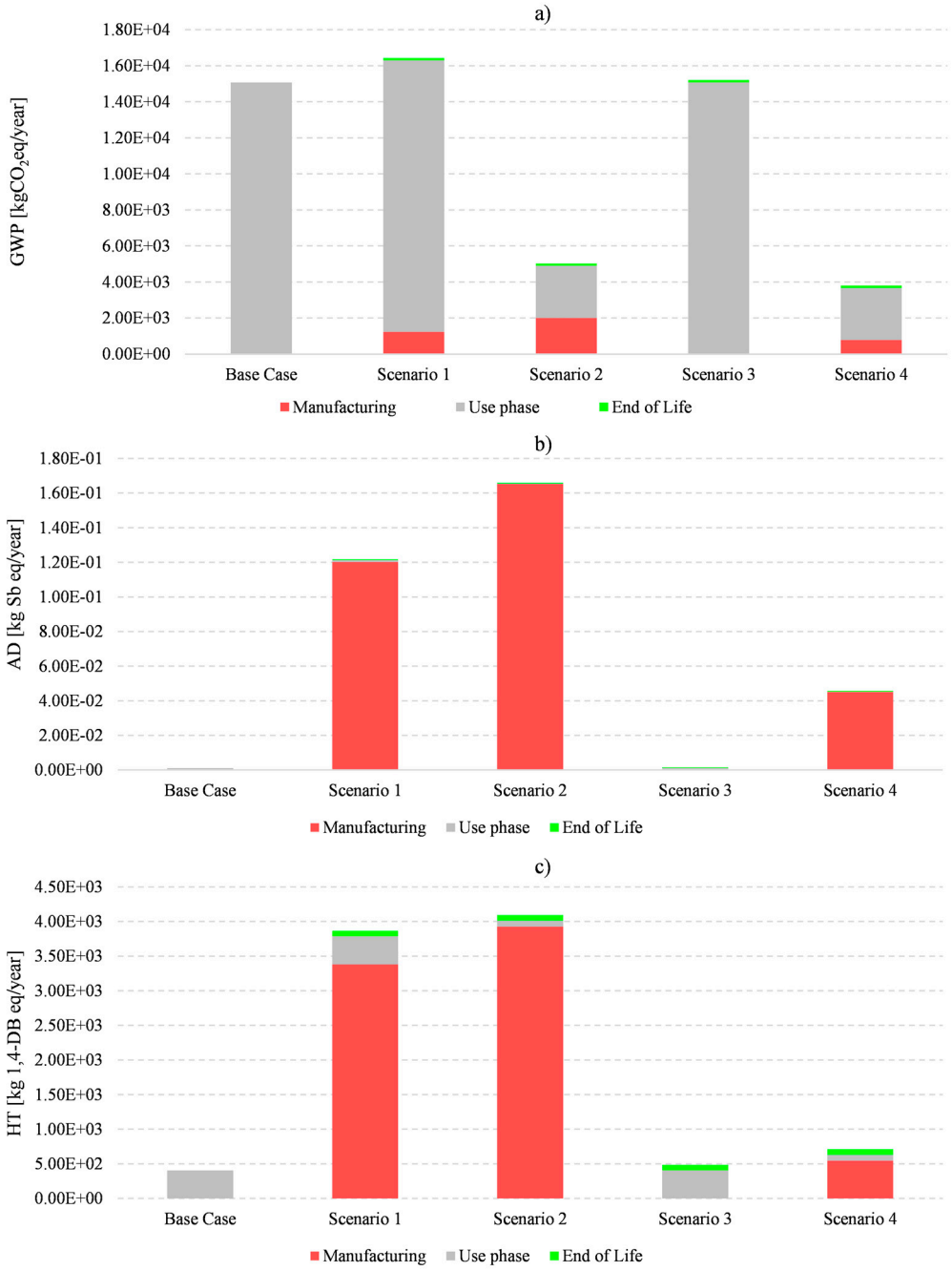

Figure 6. Life cycle impact assessment (LCIA) results in terms of global warming potential (GWP) (**a**), abiotic depletion (AD) (**b**), and human toxicity (HT) (**c**) for the considered scenarios. Results refer to the functional unit.

Finally, GWP is chosen as the metric for comparison with the existing literature as it is commonly used in LCA studies. According to Figure 6a, in this study, the contribution to GWP is primarily due to the use phase, which directly depends on the electrical consumptions indicated in Table 3. Thus, the comparison is conducted with similar studies where GWP has been calculated based on the kWh of electricity consumed. Specifically, with electrical consumptions of 32,120 kWh/y, 32,120 kWh/y, 6135 kWh/y, 32,120 kWh/y, and 6135 kWh/y for the base case, Scenario 1, Scenario 2, Scenario 3, and Scenario 4, respectively, a GWP of 1.51×10^4 $kgCO_2$ eq/y, 1.51×10^4 $kgCO_2$ eq/y, 2.88×10^3 $kgCO_2$ eq/y, 1.51×10^4 $kgCO_2$ eq/y, and 2.88×10^3 $kgCO_2$ eq/y is obtained, respectively. From these values, an average GWP value per kWh of electricity consumed is derived, amounting to

0.469 $kgCO_2$ eq/kWh. This GWP value is consistent with the literature for the average European mix, such as 0.590 $kgCO_2$ eq/kWh found in Ref. [73] and 0.334 $kgCO_2$ eq/kWh in Ref. [74], and for the worldwide average of 0.475 $kgCO_2$ eq/kWh in Ref. [75].

4. Conclusions

This study aimed to investigate the extent to which the implementation of an open-loop circular economy strategy of second-life batteries improves the sustainability of industrial applications. To this end, the authors conducted an LCA to assess and compare different settings of BESS made of new or decommissioned batteries combined with a standalone PV system serving a ball mill machine in a ceramic manufacturing plant. In particular, the study considered the following five scenarios: the base case where the ball mill machine is entirely supplied by the grid, Scenario 1 where a BESS is connected to the grid, Scenario 2 where a BESS is connected to a standalone PV system, Scenario 3 where a BESS made of decommissioned automotive batteries is connected to the grid, and Scenario 4 where a SL-BESS made of decommissioned automotive batteries is connected to a standalone PV system.

The base case reflects the contribution of the power generation mix to environmental impact indicators. Indeed, the considered generation mix heavily relies on fossil fuels, particularly coal and oil. This reliance will lead to higher climate change impact due to significant emissions of carbon dioxide during combustion and will generate pollutants like heavy metals, which can pose risks to human health through air and water contamination.

The comparative analysis of scenarios for GWP, AD, and HT with respect to the base case shows that Scenario 1 emerges as the most significant contributor to GWP, exhibiting a notably elevated value of 1.64×10^4 kg CO_2 eq. Furthermore, it demonstrates an increase in GWP of 8.61% compared with the base case, while presenting the lowest impacts across AD and HT indicators. Conversely, Scenario 2 displays the most substantial impact on both AD and HT, with values of 1.66×10^{-1} kg Sb eq. and 4.09×10^3 kg 1,4-DB eq, respectively. Notably, Scenario 2 shows a remarkable decrease in GWP, registering a reduction of approximately 66.52% relative to the base case, yet it exhibits the highest impacts in terms of AD and HT, primarily due to the manufacturing stages of BESS and PV modules. Moreover, Scenario 3 presents a marginal increase in GWP by approximately 0.66%, with moderate impacts on both AD and HT, showing rises of 44.86% and 20.05%, respectively. Finally, Scenario 4 similarly indicates a significant decrease in GWP, reaching around -74.82%.

The results suggest that the environmental benefits achieved can be extended by considering larger PV installations and SL-BESS with greater capacities. In fact, the installed PV power and the BESS capacity represent the only scalable factors, and their increase is justified by industrial plants that need to meet a higher demand for electrical energy. Similarly, regarding economic advantages, these will naturally escalate with the rise in the share of renewable energy utilized, along with the opportunity to employ greater storage capacity during periods of lower electricity prices, subsequently repurposing it during higher-cost intervals. Moreover, this study is placed within a European context, implying that resulting environmental impacts may significantly vary across different regional contexts. It is important to consider that this study utilized the average European electricity mix, which exhibits high variability among European countries. Similarly, concerning the modeling of transportation for raw materials, finished products to the site of use, and decommissioned batteries, the distances assumed align with European road infrastructure and available transportation modes in Europe. On the other hand, the regulatory framework regarding batteries and waste batteries is the same for European countries, and therefore the results can be considered consistent across them.

The results of this study contribute to the fields of renewable energy for industrial applications and the implementation of the circular economy for a product expected to be highly available in future projections. Simultaneously, the studied configuration remains aligned with the state of the art in renewable systems serving industrial applications

(e.g., Ref. [29]), taking a further step forward in the scientific research by introducing decommissioned batteries and assessing the overall environmental impact.

Future research directions could explore the optimization of the open-loop circular economy strategy by investigating the scalability of PV installations and SL-BESS capacities in industrial settings, and considering recycled materials in the manufacturing stage of Li-ion batteries and PV panels. Additionally, studies focusing on the regional variations of environmental impacts across different geographical contexts could provide valuable insights for localized implementations, such as different electricity generation mixes and centers for battery collection. Further investigations into the life cycle impacts of transportation modes for raw materials and new and decommissioned batteries, considering diverse infrastructural frameworks, would enhance the applicability of findings on a global scale. Finally, the main limitation of this study lies in its focus on decommissioned automotive batteries without considering potential variations in their condition or quality.

In conclusion, this study demonstrates the potential of the designed open-loop circular economy strategy for decommissioned automotive batteries in enhancing sustainability of industrial applications in terms of GHG emissions. Through LCA, it was possible to identify less impactful energy scenarios and discuss key environmental hotspots. The integration of renewable energy sources with BESS and SL-BESS promises to reduce GHG emissions and drive investments in green technology.

Author Contributions: Conceptualization, L.S., A.F., C.S., G.A. and D.F.; methodology, L.S., A.F., C.S., G.A. and D.F.; software, L.S., A.F., C.S., G.A. and D.F.; validation, L.S., A.F., C.S., G.A. and D.F.; formal analysis, L.S., A.F., C.S., G.A. and D.F.; investigation, L.S., A.F., C.S., G.A. and D.F.; resources, L.S., A.F., C.S., G.A. and D.F.; data curation, L.S., A.F., C.S., G.A. and D.F.; writing—original draft preparation, L.S., A.F., C.S., G.A. and D.F.; writing—review and editing, L.S., A.F., C.S., G.A. and D.F.; visualization, L.S., A.F., C.S., G.A. and D.F.; supervision, L.S., A.F., C.S., G.A. and D.F. All authors have read and agreed to the published version of the manuscript.

Funding: This research received no external funding.

Data Availability Statement: Data are contained within the article.

Conflicts of Interest: The authors declare no conflicts of interest.

References

1. Xing, M.; Luo, F.; Fang, Y. Research on the sustainability promotion mechanisms of industries in China's resource-based cities—From an ecological perspective. *J. Clean. Prod.* **2021**, *315*, 128114. [CrossRef]
2. Silvestri, L.; Forcina, A.; Di Bona, G.; Silvestri, C. Circular economy strategy of reusing olive mill wastewater in the ceramic industry: How the plant location can benefit environmental and economic performance. *J. Clean. Prod.* **2021**, *326*, 129388. [CrossRef]
3. Murray, A.; Skene, K.; Haynes, K. The Circular Economy: An Interdisciplinary Exploration of the Concept and Application in a Global Context. *J. Bus. Ethics* **2017**, *140*, 369–380. [CrossRef]
4. Gusmerotti, N.M.; Testa, F.; Corsini, F.; Pretner, G.; Iraldo, F. Drivers and approaches to the circular economy in manufacturing firms. *J. Clean. Prod.* **2019**, *230*, 314–327. [CrossRef]
5. Rajput, S.; Singh, S.P. Connecting circular economy and industry 4.0. *Int. J. Inf. Manag.* **2019**, *49*, 98–113. [CrossRef]
6. Hossain, E.; Murtaugh, D.; Mody, J.; Faruque, H.M.R.; Sunny, M.S.H.; Mohammad, N. A Comprehensive Review on Second-Life Batteries: Current State, Manufacturing Considerations, Applications, Impacts, Barriers & Potential Solutions, Business Strategies, and Policies. *IEEE Access* **2019**, *7*, 73215–73252. [CrossRef]
7. International Energy Agency, 2020. Global EV Outlook 2020. Entering the Decade of Electric Drive? Available online: https://www.iea.org/reports/global-ev-outlook-2020 (accessed on 21 August 2020).
8. Silvestri, L.; Forcina, A.; Arcese, G.; Bella, G. Recycling technologies of nickel–metal hydride batteries: An LCA based analysis. *J. Clean. Prod.* **2020**, *273*, 123083. [CrossRef]
9. Faessler, B. Stationary, Second Use Battery Energy Storage Systems and Their Applications: A Research Review. *Energies* **2021**, *14*, 2335. [CrossRef]
10. Pinegar, H.; Smith, Y.R. Recycling of End-of-Life Lithium Ion Batteries, Part I: Commercial Processes. *J. Sustain. Metall.* **2019**, *5*, 402–416. [CrossRef]
11. Global Energy & Environment Research Team. *Global Industrial Battery Market, Forecast to 2023: Growth in Renewable Energy and Distributed Generation to Drive the Global Industrial Battery Market*; Frost & Sullivan: San Antonio, TX, USA, 2018; p. 196.

12. Dunn, B.; Kamath, H.; Tarascon, J.-M. Electrical Energy Storage for the Grid: A Battery of Choices. *Science* **2011**, *334*, 928–935. [CrossRef]
13. Yang, P.; Tarascon, J.-M. Towards systems materials engineering. *Nat. Mater.* **2012**, *11*, 560–563. [CrossRef]
14. Silvestri, L.; Forcina, A.; Silvestri, C.; Traverso, M. Circularity potential of rare earths for sustainable mobility: Recent developments, challenges and future prospects. *J. Clean. Prod.* **2021**, *292*, 126089. [CrossRef]
15. Deutsche, B. *Autos & Auto Parts Electric Cars: Plugged in 2*; Deutsche Bank: Frankfurt, Germany, 2009.
16. Garole, D.J.; Hossain, R.; Garole, V.J.; Sahajwalla, V.; Nerkar, J.; Dubal, D.P. Recycle, Recover and Repurpose Strategy of Spent Li-ion Batteries and Catalysts: Current Status and Future Opportunities. *ChemSusChem* **2020**, *13*, 3079–3100. [CrossRef]
17. Zeng, X.; Li, J.; Ren, Y. Prediction of various discarded lithium batteries in China. In Proceedings of the 2012 IEEE International Symposium on Sustainable Systems and Technology (ISSST), Boston, MA, USA, 16–18 May 2012; pp. 1–4.
18. Haupt, M.; Vadenbo, C.; Hellweg, S. Do We Have the Right Performance Indicators for the Circular Economy?: Insight into the Swiss Waste Management System. *J. Ind. Ecol.* **2017**, *21*, 615–627. [CrossRef]
19. Berlin, D.; Feldmann, A.; Nuur, C. The relatedness of open- and closed-loop supply chains in the context of the circular economy; Framing a continuum. *Clean. Logist. Supply Chain* **2022**, *4*, 100048. [CrossRef]
20. Innocenzi, V.; Ippolito, N.M.; De Michelis, I.; Prisciandaro, M.; Medici, F.; Vegliò, F. A review of the processes and lab-scale techniques for the treatment of spent rechargeable NiMH batteries. *J. Power Sources* **2017**, *362*, 202–218. [CrossRef]
21. Tunsu, C.; Petranikova, M.; Gergorić, M.; Ekberg, C.; Retegan, T. Reclaiming rare earth elements from end-of-life products: A review of the perspectives for urban mining using hydrometallurgical unit operations. *Hydrometallurgy* **2015**, *156*, 239–258. [CrossRef]
22. Binnemans, K.; Jones, P.T.; Blanpain, B.; Van Gerven, T.; Yang, Y.; Walton, A.; Buchert, M. Recycling of rare earths: A critical review. *J. Clean. Prod.* **2013**, *51*, 1–22. [CrossRef]
23. Secretariat, S.P. EU SET-Plan ACTION n°7 –Declaration of Intent "Become competitive in the global battery sector to drive e-mobility forward". *Transformation* **2016**, *100*, 6317.
24. European Union. *Directive 2000/53/EC of the European Parliament and of the Council of 18 September 2000 on End-of Life Vehicles. Official Journal L*; European Union: Maastricht, The Netherlands, 2000.
25. Heymans, C.; Walker, S.B.; Young, S.B.; Fowler, M. Economic analysis of second use electric vehicle batteries for residential energy storage and load-levelling. *Energy Policy* **2014**, *71*, 22–30. [CrossRef]
26. Cusenza, M.A.; Guarino, F.; Longo, S.; Ferraro, M.; Cellura, M. Energy and environmental benefits of circular economy strategies: The case study of reusing used batteries from electric vehicles. *J. Energy Storage* **2019**, *25*, 100845. [CrossRef]
27. Silvestri, L.; De Santis, M.; Bella, G. A Preliminary Techno-Economic and Environmental Performance Analysis of Using Second-Life EV Batteries in an Industrial Application. In Proceedings of the 2022 6th International Conference on Green Energy and Applications (ICGEA), Singapore, 4–6 March 2022; pp. 99–102.
28. Silvestri, L.; De Santis, M.; Bella, G. Techno-economic Evaluation of a Second-life Battery Energy Storage System Enabling Peak Shaving and PV Integration in a Ceramic Manufacturing Plant. In Proceedings of the 2021 IEEE International Conference on Industrial Engineering and Engineering Management (IEEM), Singapore, 13–16 December 2021; pp. 1566–1570.
29. Silvestri, L.; De Santis, M. Renewable-based load shifting system for demand response to enhance energy-economic-environmental performance of industrial enterprises. *Appl. Energy* **2024**, *358*, 122562. [CrossRef]
30. Hua, Y.; Liu, X.; Zhou, S.; Huang, Y.; Ling, H.; Yang, S. Toward Sustainable Reuse of Retired Lithium-ion Batteries from Electric Vehicles. *Resour. Conserv. Recycl.* **2021**, *168*, 105249. [CrossRef]
31. Gu, X.; Bai, H.; Cui, X.; Zhu, J.; Zhuang, W.; Li, Z.; Hu, X.; Song, Z. Challenges and opportunities for second-life batteries: Key technologies and economy. *Renew. Sustain. Energy Rev.* **2024**, *192*, 114191. [CrossRef]
32. Shu, X.; Guo, Y.; Yang, W.; Wei, K.; Zhu, G. Life-cycle assessment of the environmental impact of the batteries used in pure electric passenger cars. *Energy Rep.* **2021**, *7*, 2302–2315. [CrossRef]
33. Wang, Y.; Tang, B.; Shen, M.; Wu, Y.; Qu, S.; Hu, Y.; Feng, Y. Environmental impact assessment of second life and recycling for LiFePO4 power batteries in China. *J. Environ. Manag.* **2022**, *314*, 115083. [CrossRef]
34. Ahmadi, L.; Young, S.B.; Fowler, M.; Fraser, R.A.; Achachlouei, M.A. A cascaded life cycle: Reuse of electric vehicle lithium-ion battery packs in energy storage systems. *Int. J. Life Cycle Assess.* **2017**, *22*, 111–124. [CrossRef]
35. Hendrickson, T.P.; Kavvada, O.; Shah, N.; Sathre, R.; Scown, C.D. Life-cycle implications and supply chain logistics of electric vehicle battery recycling in California. *Environ. Res. Lett.* **2015**, *10*, 14011. [CrossRef]
36. Raugei, M.; Winfield, P. Prospective LCA of the production and EoL recycling of a novel type of Li-ion battery for electric vehicles. *J. Clean. Prod.* **2019**, *213*, 926–932. [CrossRef]
37. Dunn, J.B.; Gaines, L.; Kelly, J.C.; James, C.; Gallagher, K.G. The significance of Li-ion batteries in electric vehicle life-cycle energy and emissions and recycling's role in its reduction. *Energy Environ. Sci.* **2015**, *8*, 158–168. [CrossRef]
38. Rajaeifar, M.A.; Raugei, M.; Steubing, B.; Hartwell, A.; Anderson, P.A.; Heidrich, O. Life cycle assessment of lithium-ion battery recycling using pyrometallurgical technologies. *J. Ind. Ecol.* **2021**, *25*, 1560–1571. [CrossRef]
39. Peters, J.F. Best practices for life cycle assessment of batteries. *Nat. Sustain.* **2023**, *6*, 614–616. [CrossRef]
40. Ember Climate. 2023. Available online: https://ember-climate.org/insights/research/european-electricity-review-2023/ (accessed on 28 March 2024).

41. Bin Wali, S.; Hannan, M.A.; Reza, M.S.; Ker, P.J.; Begum, R.A.; Rahman, M.S.A.; Mansor, M. Battery storage systems integrated renewable energy sources: A biblio metric analysis towards future directions. *J. Energy Storage* **2021**, *35*, 102296. [CrossRef]
42. Venettacci, S.; Cozzolino, R.; Ponticelli, G.S.; Guarino, S. Environmental and economic life cycle assessment of thermal energy storage based on organic phase change material embedded in open-cell copper foams. *Sustain. Prod. Consum.* **2022**, *29*, 387–405. [CrossRef]
43. Neumann, J.; Petranikova, M.; Meeus, M.; Gamarra, J.D.; Younesi, R.; Winter, M.; Nowak, S. Recycling of Lithium-Ion Batteries—Current State of the Art, Circular Economy, and Next Generation Recycling. *Adv. Energy Mater.* **2022**, *12*, 2102917. [CrossRef]
44. Han, X.; Li, Y.; Nie, L.; Huang, X.; Deng, Y.; Yan, J.; Kourkoumpas, D.-S.; Karellas, S. Comparative life cycle greenhouse gas emissions assessment of battery energy storage technologies for grid applications. *J. Clean. Prod.* **2023**, *392*, 136251. [CrossRef]
45. Gandiglio, M.; Marocco, P.; Bianco, I.; Lovera, D.; Blengini, G.A.; Santarelli, M. Life cycle assessment of a renewable energy system with hydrogen-battery storage for a remote off-grid community. *Int. J. Hydrogen Energy* **2022**, *47*, 32822–32834. [CrossRef]
46. Silvestri, L.; Forcina, A.; Arcese, G.; Bella, G. Environmental Analysis Based on Life Cycle Assessment: An Empirical Investigation on the Conventional and Hybrid Powertrain. In *Proceedings of the Conference on Sustainable Mobility*; SAE International: Warrendale, PA, USA, 2019.
47. de Souza, L.L.P.; Lora, E.E.S.; Palacio, J.C.E.; Rocha, M.H.; Renó, M.L.G.; Venturini, O.J. Comparative environmental life cycle assessment of conventional vehicles with different fuel options, plug-in hybrid and electric vehicles for a sustainable transportation system in Brazil. *J. Clean. Prod.* **2018**, *203*, 444–468. [CrossRef]
48. Peña, C.; Civit, B.; Gallego-Schmid, A.; Druckman, A.; Pires, A.C.; Weidema, B.; Mieras, E.; Wang, F.; Fava, J.; Canals, L.M.i.; et al. Using life cycle assessment to achieve a circular economy. *Int. J. Life Cycle Assess.* **2021**, *26*, 215–220. [CrossRef]
49. Spreafico, C. An analysis of design strategies for circular economy through life cycle assessment. *Environ. Monit. Assess.* **2022**, *194*, 180. [CrossRef]
50. *UNI EN ISO 14040:2006*; Environmental Management—Life Cycle Assessment—Principles and Framework. International Organization for Standardization: Geneva, Switzerland, 2006.
51. *ISO 14044:2006/Amd 1:2017*; Environmental Management—Life Cycle Assessment—Requirements and Guidelines—Amendment 1. International Organization for Standardization: Geneva, Switzerland, 2006.
52. Guinée, J.B.; Gorrée, M.; Heijungs, R.; Huppes, G.; Kleijn, R.; De Koning, A.; Van Oers, L.; Sleeswijk, A.W.; Suh, S.; de Haes, H.A.; et al. *Life Cycle Assessment—An Operational Guide to the ISO Standards—Part 3: Scientific Background*; Ministry Housing, Spatial Planning Environmental Center Environmental Science (CML): Den Haag Leiden, The Netherlands, 2001.
53. Guinée, J.B.; Gorrée, M.; Heijungs, R.; Huppes, G.; Kleijn, R.; De Koning, A.; Van Oers, L.; Wegener Sleeswijk, A.; Suh, S.; de Haes, H.A.; et al. *Life Cycle Assessment; An Operational Guide to the ISO Standards; Parts 1 and 2*; Ministry Housing, Spatial Planning Environmental Center Environmental Science (CML): Den Haag Leiden, The Netherlands, 2001.
54. PRé-Consultants. *LCA Software and Database Manual*; PRé Sustainability: Amersfoort, The Netherlands, 2014.
55. Ecoinvent. The LifeCycle Inventory Data, Version 3.9.1. Swiss Centre for Life CycleInventories. In *Proceedings of the Swiss Centre for Life Cycle Inventories*; Ecoinvent: Duebendorf, Switzerland, 2023.
56. SimaPro. SimaPro Database Manual—Methods Library; SimaPro: 2018. Available online: https://simapro.com/wp-content/uploads/2022/07/DatabaseManualMethods.pdf (accessed on 28 March 2024).
57. Zeng, A.; Chen, W.; Rasmussen, K.D.; Zhu, X.; Lundhaug, M.; Müller, D.B.; Tan, J.; Keiding, J.K.; Liu, L.; Dai, T.; et al. Battery technology and recycling alone will not save the electric mobility transition from future cobalt shortages. *Nat. Commun.* **2022**, *13*, 1341. [CrossRef] [PubMed]
58. Majeau-Bettez, G.; Hawkins, T.R.; Strømman, A.H. Life Cycle Environmental Assessment of Lithium-Ion and Nickel Metal Hydride Batteries for Plug-In Hybrid and Battery Electric Vehicles. *Environ. Sci. Technol.* **2011**, *45*, 4548–4554. [CrossRef] [PubMed]
59. Tytgat, J. *Umicore—Recycling of NiMH and Li-Ion Batteries a Sustainable New Business*; Wiley: Hoboken, NJ, USA, 2011.
60. Morel, H. Ultra High Temperature (UHT) Technology at Technology at Umicore. 2010. Available online: http://www.lusitana.umicore.com/img/uploads/irpresentations/35/2010CMD_UHT.pdf (accessed on 28 March 2024).
61. Silvestri, L.; Forcina, A.; Silvestri, C.; Ioppolo, G. Life cycle assessment of sanitaryware production: A case study in Italy. *J. Clean. Prod.* **2020**, *251*, 119708. [CrossRef]
62. Photovoltaic Geographical Information System. PVGIS (C). 2023. Available online: https://re.jrc.ec.europa.eu/pvg_tools/en/ (accessed on 28 March 2024).
63. Lv, J.; Wang, Z.; Ma, S. Calculation method and its application for energy consumption of ball mills in ceramic industry based on power feature deployment. *Adv. Appl. Ceram.* **2020**, *119*, 183–194. [CrossRef]
64. Fragoso, A.; Martins, R.F.; Soares, A.C. Failure analysis of a ball mill located in a cement's production line. *Eng. Fail. Anal.* **2022**, *138*, 106339. [CrossRef]
65. Little, L.; Mainza, A.N.; Becker, M.; Wiese, J. Fine grinding: How mill type affects particle shape characteristics and mineral liberation. *Miner. Eng.* **2017**, *111*, 148–157. [CrossRef]
66. Zhang, Y.; Ma, S.; Yang, H.; Lv, J.; Liu, Y. A big data driven analytical framework for energy-intensive manufacturing industries. *J. Clean. Prod.* **2018**, *197*, 57–72. [CrossRef]
67. Ma, S.; Zhang, Y.; Liu, Y.; Yang, H.; Lv, J.; Ren, S. Data-driven sustainable intelligent manufacturing based on demand response for energy-intensive industries. *J. Clean. Prod.* **2020**, *274*, 123155. [CrossRef]

68. Li, H.; Yang, H.; Yang, B.; Zhu, C.; Yin, S. Modelling and simulation of energy consumption of ceramic production chains with mixed flows using hybrid Petri nets. *Int. J. Prod. Res.* **2018**, *56*, 3007–3024. [CrossRef]
69. Shi, F.; Xie, W. A specific energy-based ball mill model: From batch grinding to continuous operation. *Miner. Eng.* **2016**, *86*, 66–74. [CrossRef]
70. Xu, B.; Oudalov, A.; Ulbig, A.; Andersson, G.; Kirschen, D.S. Modeling of Lithium-Ion Battery Degradation for Cell Life Assessment. *IEEE Trans. Smart Grid* **2018**, *9*, 1131–1140. [CrossRef]
71. Colucci, R.; Mahgoub, I.; Yousefizadeh, H.; Al-Najada, H. Survey of Strategies to Optimize Battery Operation to Minimize the Electricity Cost in a Microgrid With Renewable Energy Sources and Electric Vehicles. *IEEE Access* **2024**, *12*, 8246–8261. [CrossRef]
72. Fthenakis, V.M.; Kim, H.C. Life cycle assessment of high-concentration photovoltaic systems. *Prog. Photovolt. Res. Appl.* **2013**, *21*, 379–388. [CrossRef]
73. Warrier, G.A.; Palaniappan, S.; Habert, G. Classification of sources of uncertainty in building LCA. *Energy Build.* **2024**, *305*, 113892. [CrossRef]
74. Scarlat, N.; Prussi, M.; Padella, M. Quantification of the carbon intensity of electricity produced and used in Europe. *Appl. Energy* **2022**, *305*, 117901. [CrossRef]
75. Iranshahi, K.; Rubinetti, D.; Onwude, D.I.; Psarianos, M.; Schlüter, O.K.; Defraeye, T. Electrohydrodynamic drying versus conventional drying methods: A comparison of key performance indicators. *Energy Convers. Manag.* **2023**, *279*, 116661. [CrossRef]